Current Research in Food Science 4 (2021) 698–706

Contents lists available at ScienceDirect

Current Research in Food Science

journal homepage: www.sciencedirect.com/journal/current-research-in-food-science

Research Paper

Alginate-based microparticles structured with different biopolymers and enriched with a phenolic-rich olive leaves extract: A physico-chemical characterization

Federica Flamminii [a], Maria Paciulli [b], Alessandro Di Michele [c], Paola Littardi [b], Eleonora Carini [b], Emma Chiavaro [b], Paola Pittia [a], Carla Daniela Di Mattia [a,*]

[a] Faculty of Bioscience and Technology for Agriculture, Food and Environment, University of Teramo, Via Balzarini 1, 64100, Teramo, Italy
[b] Department of Food and Drug, University of Parma, Parco Area Delle Scienze 27/A, 43124, Parma, Italy
[c] Department of Physics and Geology, University of Perugia, Via Pascoli, 06123, Perugia, Italy

ARTICLE INFO

Keywords:
Olive leaves polyphenols
Encapsulation
Alginate beads
Microstructure
Differential scanning calorimetry

ABSTRACT

Encapsulation of olive leaves extracts (OLE), rich of healthy components like Oleuropein, Hydroxytyrosol and Verbascoside, represents a new challenge to improve stability and nutritional value of food as well as a way to recover value added compounds from by-products, contributing to a more sustainable food system. In this context, OLE-loaded microbeads of Na alginate alone or in combination with Pectin, Na Caseinate or Whey protein isolates, were produced by emulsification internal ionotropic gelation. Encapsulation efficiency of the main phenolic compounds (Oleuropein, Hydroxytyrosol, Verbascoside) was carried out along with microparticles morphological characterization by scanning electron microscopy (SEM), thermal properties by differential scanning calorimetry (DSC) and color. Encapsulation efficiency resulted higher for Alginate/Pectin, whilst Alginate/Caseinate was the less performing system, probably due to the lower interaction with polyphenols. SEM revealed collapsed structures and continuous smooth surfaces for Alginate and Alginate/Pectin microbeads while more regular structures and porous surfaces were observed for Alginate/Caseinate and Alginate/Whey proteins. Higher hue angle and lower chroma values were observed for all the beads with respect to the pure extract, indicating a reduction of the yellow/brown color. DSC highlighted higher thermal stability for the microbeads in comparison to the original ingredients, showing also new thermal transitions related to bonds formation between polymers and OLE.

1. Introduction

Antioxidants, antimicrobials, aromas and pigments recovered from by-products are value added compounds of great interest for the food industry; however, they are quite often characterized by poor solubility, high sensitivity to environmental stresses (T, pH, light, oxygen, moisture) and easily undergo degradation during gastrointestinal digestion, with negative consequences on their bioavailability and bioactivity. Microencapsulation can represent a promising tool as it can provide the bio-compounds with an appropriate protection towards instability phenomena and increase their potential application. For microencapsulation purposes different technologies are available, such as spray drying, freeze drying, coacervation, liposomes, ionic gelation, emulsions and many others, well described and detailed in many reviews (Fang and Bhandari, 2010; Lu et al., 2016; McClements, 2017; Ozkan et al., 2019). The choice of a specific methodology should consider the aim of the encapsulation, the nature of the compounds, the materials used as carrier system, the size of the microparticles and the final applications. All these factors led to the development of different delivery systems, with peculiar physicochemical characteristics, that need to be studied in detail to allow their exploitation as functional ingredients.

With regards to the carrier systems, several natural polymers like alginate, pectin, guar gums or chitosan have been proposed as encapsulating agents for different active compounds, for both foods and pharmaceutical applications (Kurozawa and Hubinger, 2017; Osojnik Črnivec and Poklar Ulrih, 2019). Alginate, a linear copolymer made of D-mannuronic and L-guluronic acids obtained mainly from marine algae and some bacteria, is one of the most widely used materials for the

* Corresponding author.
E-mail address: cdimattia@unite.it (C.D. Di Mattia).

https://doi.org/10.1016/j.crfs.2021.10.001
Received 21 April 2021; Received in revised form 2 October 2021; Accepted 4 October 2021
Available online 6 October 2021

encapsulation of many bioactive compounds as it is food grade, cheap, and biocompatible; it exerts superior gelling properties under safe and mild conditions, suitable for thermosensitive molecules and it is widely used to form particles apt for food applications (Ching et al., 2017). The formation of the gel structure is driven by divalent cations, mainly Ca^{2+}, which bind the guluronate moieties of the alginate polymer chains, forming what it is largely described in literature as an 'egg-box' structure (Leong et al., 2016). However, depending on alginate properties (i.e. molecular weight, mannuronic acid/guluronic acid ratio) and processing factors (i.e. type of gelation, type of cation and concentration), alginate gel particles show various porosity and permeability, leading to different molecules diffusion kinetics with possible drawbacks in their exploitation in food matrices (Córdoba et al., 2014). This limit can be overcome through the combination of alginate with other polymers, proteins or polysaccharides, that can act either as wall material (e.g. chitosan) (Belščak-Cvitanović et al., 2015), or as filling agents (e.g. starch, pectin, whey protein isolate, inulin, arabic gum, etc.). These latter act by reinforcing the hydrogel structure through interactions among the bioactive compounds, alginate and the co-structurants themselves (Bušić et al., 2018; Córdoba et al., 2014; Flamminii et al., 2020a; Pacheco et al., 2018).

In the last years, alginate-based microcapsules have been successfully developed and tested for the encapsulation of added value compounds recovered from agro-industrial by-products in order to reduce the waste and valorize compounds which may be useful for the development of nutraceuticals and functional food additives (Kurozawa and Hubinger, 2017).

Among plant by-products, olive leaves and their extracts contain the highest amount of phenolic compounds, especially with respect to other olive by-products (Difonzo et al., 2017; Hassen et al., 2015; Roselló-Soto et al., 2015) whose composition can be affected by biotic and abiotic agronomical factors (Flamminii et al., 2020b). The main phenolic groups represented in olive leaves are secoiridoids, flavonoids and simple phenols. Oleuropein, from the first group, is quantitatively the most abundant with amounts ranging from 60 to 90 mg/g of dry weight, while Verbascoside and Ligstroside are generally present in lower proportions. Among flavonoids and simple phenols, the most represented compounds are Luteolin-7-glicoside and Hydroxytyrosol, respectively.

Beside the health effects, microparticles loaded with phenolic-rich extracts can also act as high-tech additives and preservatives for the formulation of complex food systems, improving the dispersion degree of emulsified matrices and extending foodstuff shelf-life (Paulo and Santos, 2020). In this context, the use of olive phenolic compounds encapsulated in different structures, as antioxidants and structuring ingredients in various food matrices, has been the goal of several recent researches (Flamminii et al., 2020b; Ganje et al., 2016; Jolayemi et al., 2021; Mohammadi et al., 2016; Robert et al., 2019; Tavakoli et al., 2018).

Alginate-based microparticles formulated with different polymers (alginate, alginate-pectin, alginate-whey proteins isolate and alginate-sodium caseinate) and enriched with olive leaves phenolic extract (OLE) were investigated in a previous study from our research group; the encapsulation efficiency by total phenolic content, particle size, swelling and release kinetics in two different media (pH 4.5 and 6), antioxidant capacity and polymers-polyphenols interaction by FT-IR analysis were evaluated (Flamminii et al., 2020a). In this new research step, considered as a follow-up of the prior study, the physico-chemical characterization of alginate-based microparticles (alginate, alginate-pectin, alginate-whey proteins isolate and alginate-sodium caseinate), enriched with OLE, was completed by testing microstructure by Scanning Electron Microscopy (SEM), thermal properties by Differential Scanning Calorimetry (DSC) and color indices, in order to drive the correct use of these innovative ingredients in the formulation of foods. In particular, the DSC measurements provided an insight into the putative thermal stability of the differently formulated alginate beads and of the encapsulated bioactive compounds under heating conditions which can mimic some common food processing operations. On the other hand, the encapsulation efficiency by monitoring selected specific phenolic compounds was useful to study their partitioning behaviour that might further affect their technological functionality when added in complex food systems, such as a different efficiency in retarding oxidative phenomena in enriched food matrices as well as, from a sensory viewpoint, a different masking effect of any unpleasant bitter perception usually associated to phenolic compounds.

2. Materials and methods

2.1. Materials

Sodium alginate (W201502, Lot# MKBP8122V), sodium caseinate, calcium citrate, glacial acetic acid, Tween 20 and Span 80 were purchased from Sigma-Aldrich (St. Luis, USA). Pectin citrus (methoxy groups $\leq$6.7%) was obtained from Alfa Aesar (Kandel, Germany); whey protein isolate (WPI) (SuperproteinTM Clear 895, 90% protein) was produced by Fonterra (Auckland City, New Zealand) and kindly provided by UNIVAR (Milan, Italy). Sunflower oil was purchased in a local market. Olive leaves extract (OLE), extracted with ethanolic-aqueous maceration from leaves of the olive tree (Olea europaea L.), was kindly provided by OLEAFIT S.r.l. (Isola del Gran Sasso, Italy).

2.2. Alginate microparticles preparation

Alginate microparticles were produced by an emulsification internal ionotropic gelation technique as reported by Flamminii et al. (2020a), following the 'enriched' procedure. Briefly, encapsulant solutions, alginate (2% w/v) in combination either with pectin (2% w/v), or whey proteins (2% w/v) or sodium caseinate (2% w/v) and enriched with 0.5% (w/v) OLE, were prepared using an Ultra-Turrax model T25 Basic (Ika- Werke GmbH & Co, Germany) until complete dissolution and stored overnight under refrigeration to allow complete hydration and deareation. Twenty grams of the polymeric aqueous solution were mixed with 1 mL of a suspension of calcium citrate eptahydrate (500 mM Ca^{2+} equivalents) and dispersed for 15 min by means of a magnetic stirrer in 100 g of sunflower oil containing 2% (w/w) Span 80. Twenty milliliters of sunflower oil with 500 μL glacial acetic acid were added to the water-in-oil emulsion and stirred for 30 min. The gelled microparticles were then separated by adding 150 mL of 0.05 M $CaCl_2$ with 0.5% (w/v) Tween 20 and 0.5% (w/v) phenolic extracts, gently agitated for 30 min until complete particles partitioning. After centrifugation (1000 rpm; 5 min) the oil was removed by aspiration and the gelled microbeads were recovered under vacuum filtration and washed with 30 mL of 70% ethanol solution with 0.5% (w/v) phenolic extracts to remove oil traces. Four different sets of enriched microparticles where produced: alginate (Alg) alginate/pectin (Alg/Pec), alginate/whey protein isolate (Alg/WPI) and alginate/caseinate (Alg/Cas).

Particles with no OLE (blank) added in the encapsulant solutions were also prepared and used as control. The particle size of OLE-enriched microbeads, expressed as $D_{4,3}$, ranged from 48 μm to 65 μm. The beads were frozen at −40 °C, let to freeze-dry for 24 h at −90 °C and stored at room temperature in desiccator over silica gel and in dark conditions until analysis.

2.3. Phenolic compounds partitioning

Encapsulation efficiency and partitioning behaviour of the main OLE phenolic compounds into alginate microparticles were assessed by HPLC-DAD. OLE loaded alginate microparticles were initially dissolved with 10% (w/v) sodium citrate solution (Flamminii et al., 2020a). The solution containing the broken microbeads was properly centrifuged at 13,000 rpm for 5 min, diluted and filtered with 0.22 mm nylon filters prior the injection into the chromatographic system. The elution was conducted by an Agilent 1200 series HPLC device (Agilent, Santa Clara,

USA) with a photodiode array detector (Agilent, Santa Clara, USA). The separation was performed on a Kinetex C18, (250 mm length x 4,6 mm i. d, 5 μm particle size) using a mobile phase consisting of (A) acetic acid 2.5% (v/v) and (B) acetonitrile at a constant flow rate of 0.8 ml/min in a gradient mode. Chromatograms were acquired at 280 nm for Oleuropein and Hydroxytyrosol and 330 nm for Verbascoside which were used as standards for the preparation of the calibration curves. Results were expressed as mg of standard/mg of microparticle powder as dry matter (dm). Encapsulation efficiency (EE%) for each phenolic compound (pc) was evaluated as follow (Eq. (1)):

$$EE\% = (mg_{pc}/mg_{dm})_{cs} / (mg_{pc}/mg_{dm})_{is}*100 \quad (1)$$

were $(mg_{pc}/mg_{dm})_{cs}$ represent the phenolic content of the citrate solution (cs) and $(mg_{pc}/mg_{dm})_{is}$ represent the phenolic content of the initial encapsulant solution (is).

2.4. Scanning electron microscopy (SEM) analysis

The microstructure of the freeze-dried microparticles and their surface morphology were assessed by using a field-emission scanning electron microscope (FE-SEM) LEO 1525 (ZEISS, Germany) reported by González-Ortega et al. (2020) with slight modifications. Prior to image acquisition, sample powders were immobilized on stubs and coated with a thin layer of chromium (8 nm). Acceleration potential voltage was maintained at 5 kV.

2.5. Color

The color of the microparticles was evaluated with a CHROMA METER CR5 instrument (Konica Minolta, Japan), illuminant D65; an amount of powder sample was homogeneously distributed into a glass vessel and the color was recorded in three different points. The average of the three measurements was assessed for all the colorimetric parameters (L*, a* and b*). a* and b* parameters were used to calculate the tonality angle (Hue angle, h°) and the chroma (C^{*}) according to equations (2) and (3), respectively.

$$h^{\circ} = tan^{-1}\left(\frac{b^{*}}{a^{*}}\right) \quad (2)$$

$$C^{*} = \sqrt{(a^{*})^{2} + (b^{*})^{2}} \quad (3)$$

2.6. Thermal analysis

Thermal analysis was conducted by DSC Q100 (TA Instruments, New Castle, DE, USA) on the original powdered ingredients (INGR), the freeze-dried blank gels (blank), and the freeze-dried microbeads containing the phenolic extract. Eight to 10 mg of each sample were accurately weighted with an analytical scale (Ohaus AR2140, Florham Park, Nj, USA) into stainless steel pans (PerkinElmer, Waltham, MA, USA), hermetically sealed and then analyzed. An empty pan was used as reference. Samples and reference pans were equilibrated at 25 °C for 2 min and then heated to 350 °C at a scanning rate of 10 °C/min. Dry nitrogen was purged in the DSC cell at 50 mL min^{-1}. Indium (melting temperature 156.6 °C, ΔHm = 28.71 J g^{-1}) and mercury (melting temperature − 38.83 °C, ΔHm = 11.41 J g^{-1}) were used to calibrate the instrument. The thermograms were analyzed by the Software Universal Analysis (Version 3.9 A, TA Instruments) to obtain onset temperature of transition (T_{on}, °C), peak temperature at the maximum (T_p), offset temperature of transition (T_{off}, °C) and enthalpy change for transition (ΔH, J g^{-1}). Glass transition temperature (Tg) was recorded as the T_{on} of the corresponding transition. Three replicates were analyzed per sample, and data were tabulated as average value ± standard deviation.

2.7. Statistical analysis

All experiments were carried out at least in triplicate on each of the three independent batches of production; results were reported as mean and standard deviation. A one-way analysis of variance (ANOVA) and Tukey's test were used to establish the significance of differences among the mean values at the 0.05 significance level; statistically significant differences were indicated by using different letters, with "a" assigned to the highest value of the data set and the other letters to decreasing values by following alphabetic order. Data analysis and modelling were carried out by XLSTAT software (Addinsoft SARL, New York, USA).

3. Results and discussion

3.1. Phenolic compounds partitioning and encapsulation efficiency

The present investigation focused the attention on the two most abundant secoiridoids found in olive leaves and olive leaves phenolic extracts, Oleuropein and Verbascoside (Fig. 1), as confirmed by the preliminary HPLC characterization carried out on the extract used in the work (data not shown). Despite its low amount in olive leaves, the content of Hydroxytyrosol was also investigated because, besides being generally used as reference compound in olive derivatives for its high antioxidant activity, it is also a degradation product of both Oleuropein and Verbascoside.

The content of Oleuropein, Hydroxytyrosol and Verbascoside is reported in Table 1. As expected, Oleuropein represented the main phenolic compound followed by Verbascoside and Hydroxytyrosol. In order to study the effect of the different co-structurants on the retention and partitioning of the main phenolic compounds, results were normalized on the amount of each initial encapsulant solution and reported as encapsulation efficiency, expressed as % (Fig. 2).

The type of carrier system, and in particular the polymer used, significantly ($p < 0.05$) affected the encapsulation efficiency. Alg/Pec microparticles generally accounted for the highest encapsulation efficiency among the systems, followed by Alg/WPI, Alg and Alg/Cas, respectively. With respect to the amount in the initial encapsulant solutions, that were standardized to a fixed concentration, the encapsulation procedure led to a general decrease of the content of each phenolic compound. This reduction can be partially related to the diffusive phenomena which take place during the gelation procedure from the inner matrix to the outer solution and can be generally associated to the porosity of the alginate gel structure (Ching et al., 2017; Kurozawa and Hubinger, 2017). The addition of pectin as co-structurant improved the encapsulation efficiency of Oleuropein (70%) and Verbascoside (100%), with respect to the other systems, but with no

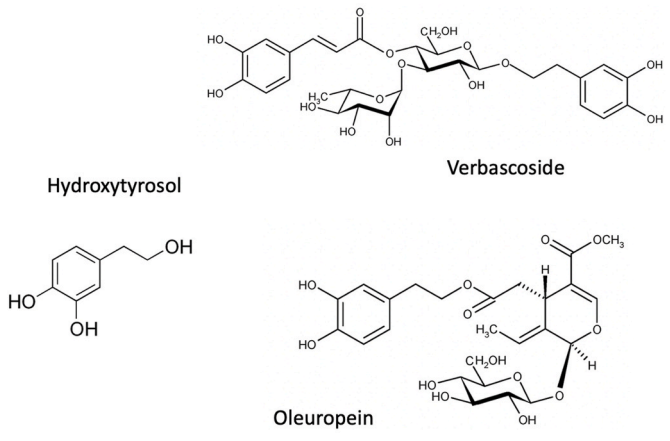

Fig. 1. Chemical structures of some phenolic compounds found in olive leaves extract.

Table 1
Concentration of the specific phenolic compounds retained in the microbeads.

	Oleuropein mg/g_{dm}	Hydroxytyrosol mg/g_{dm}	Verbascoside mg/g_{dm}
Alg	55.08 ± 2.18^{b}	1.06 ± 0.06^{a}	2.36 ± 0.36^{a}
Alg/Pec	62.13 ± 2.21^{a}	0.26 ± 0.01^{b}	3.11 ± 0.39^{a}
Alg/WPI	49.88 ± 2.86^{b}	0.18 ± 0.01^{bc}	2.68 ± 0.40^{a}
Alg/Cas	33.22 ± 2.13^{c}	0.14 ± 0.01^{c}	1.32 ± 0.05^{b}

Results are expressed as mg/g_{dm} of microparticles. Different letters in the same column highlight significant statistical differences at $p < 0.05$.

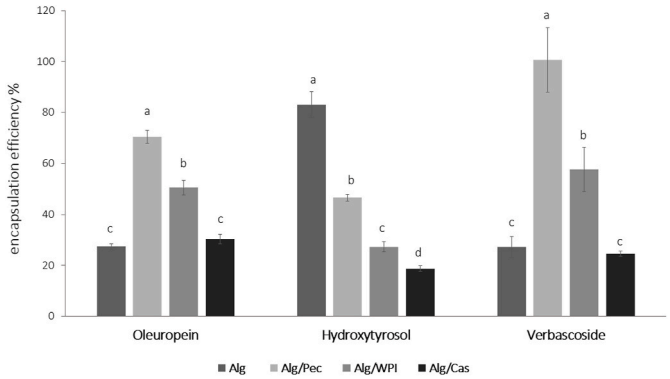

Fig. 2. Encapsulation efficiency (%) of specific phenolic compounds in the different microparticles (Alg: Alginate; Alg/Pec: Alginate/Pectin; Alg/WPI: Alginate/Whey Protein Isolate; Alg/Cas: Alginate/Caseinate). Different letters for the same phenolic compound highlight statistical significant differences at $p < 0.05$.

improvements on Hydroxytyrosol (47%) that, unexpectedly, resulted better entrapped in the matrix made only of alginate (83%), showing, in the case, a detrimental effect of any of the co-structurants tested. When compared to the control gels made by alginate alone, no significant effects were found on the encapsulation efficiency of Oleuropein and Verbascoside when casein was added to the systems. On the contrary, the use of WPI as costructurant affected the encapsulation efficiency of each phenolic compound. Indeed, results showed significant effect ($p < 0.05$) in the Alg/WPI system over the retention of phenolic compounds with values reaching 51, 27 and 58% for Oleuropein, Hydroxytyrosol and Verbascoside, respectively. These results can be ascribed to the fact that, in the alginate systems enriched with proteins, the phenolic extract interacted more with the carbohydrate moiety with respect to the protein one, as evidenced in our previous study by FT-IR analyses (Flamminii et al., 2020a), causing a lower encapsulation efficiency, especially in the Alg/Cas systems. Moreover, as proteins are capable of ionic interactions, they can also bind with polymers that have free carboxylic end groups, leading to a reduction of available free binding group (Jyothi et al., 2010).

According to previous results, binary mixtures of alginate in combination with polysaccarides or proteins are effective in improving the retention of specific phenolic compounds, thought different mechanisms, with respect of Alginate alone (Flamminii et al., 2020a; Li et al., 2021). The differences in the encapsulation efficiency among the systems could be related also to the different chemical structure of the phenolic compounds (Fig. 1), where the presence of hydroxyl groups favoured the formation of hydrogen bonds with free carboxyl end groups of proteins and polysaccarides (Li et al., 2009). OLE was indeed proven to weaken the O–H bond as its frequency stretching down-shifts at lower energy, which is an effect suggesting that the molecular interactions were formed via hydrogen bonding. Moreover, the higher amount of hydroxyl residues may also explain why verbascoside generally showed increased values of encapsulation efficiency when compared to Oleuropein (Flamminii et al., 2020a). These results are in agreement with data of other similar studies on polyphenols of *Taraxacum officinale* L. encapsualted in natural fillers, such as whey protein, cocoa powder and carob (Bušić et al., 2018), or encapsulated in alginate and pectin hydrogels reinforced by whey proteins and hydroxypropyl methylcellulose (Belščak-Cvitanovic et al., 2016). Actually, in both these studies the encapsulation efficiency of specific phenolic compounds was dependent on the carrier material added to the alginate network.

3.2. Beads morphology by SEM

The SEM images (Fig. 3) of the freeze dried microparticles allowed the characterization of the shape and surface morphology of the differently formulated alginate beads.

Freeze-drying modifies the morphological aspect of cross-linked alginate beads highlighting irregular shapes and heteogeneous surfaces (Belščak-Cvitanovic et al., 2016; Bušić et al., 2018; Córdoba et al., 2014). In our study, the drying step highly affected the shape of all the samples, in particular those obtained with alginate alone (Alg, Fig. 3a) and alginate/pectin (Alg/Pec, Fig. 3c), with a more marked collapsed structure and a red blood cell shape. The addition of proteins to the alginate matrix improved the stability of the gel network over the drying process, acting as structural support against beads shrinking and collapse during drying. In particular, alginate combined with whey protein isolate (Alg/WPI, Fig. 3e) or sodium caseinate (Alg/cas, Fig. 3g) showed a more spherical or slightly oval shape and reduced or even no structure collapse at all was observed. As for the shape, the type of polymer used highly affected microparticles surface morphology. Alg and Alg/Pec sample (Fig. 3b and d) showed an heterogenous profile with a thick and continuous structure; samples prepared with proteins (Alg/WPI and Alg/Cas, Fig. 3f and h) showed a marked irregular, rough and porous surface. Despite the differences in the polymer used, all the microparticles showed quite similar size in dried state (≈6 μm).

3.3. Thermal analysis

DSC analysis was conducted with the aim to study the thermal behaviour of the encapsulating systems in a range of temperature 25–350 °C. Information related to the formation of new complexes between the different components was also explored. Fig. 4 shows the thermograms of the powder ingredients before gelation (Fig. 4a), the freeze-dried blank particles (Fig. 4b) and the OLE-enriched microbeads (Fig. 4c), while Table 2, Table 3 and Table 4 report the characteristic temperatures and enthalpies of the observed thermal events, as endothermic, exothermic and glass transitions of the powder ingredients before gelation, blank and OLE enriched microbeads, respectively. The analysis was conducted on the freeze dried microbeads, being it the stabilized form for the final use.

All ingredients showed (Fig. 4a) a broad endothermic peak (*a*), with a Ton at ca. 30 °C and peak temperatures ranging from 78 °C to ca. 90 °C for of WPI_Ingr and Pec_Ingr, respectively (Table 2). This phenomenon was previously attributed to the loss of water associated to hydrophilic groups of polymers (Belščak-Cvitanovic et al., 2016; Elzoghby et al., 2013).

At temperature above 100 °C, a different behaviour was observed for the various ingredients, according to their nature. The olive leaf extract (Estr_Ingr) showed a small endothermic transition with a maximum peak at around 124 °C (*b*) and with an enthalpy of ≈1.3 J g^{-1} (Table 2). In a work in which crude olive leaves extract was studied by DSC, an endothermic peak at 175 °C, attributed to the melting point of oleuropein, was observed (Mourtzinos et al., 2007). The different temperature observed in this study may be due to a diverse composition of the extract or the presence of water, presumably not detected by the other authors.

Alg_Ingr and Pec_Ingr showed a similar thermal behaviour, with an almost flat profile until ca. 200 °C; an exothermic peak with a maximum

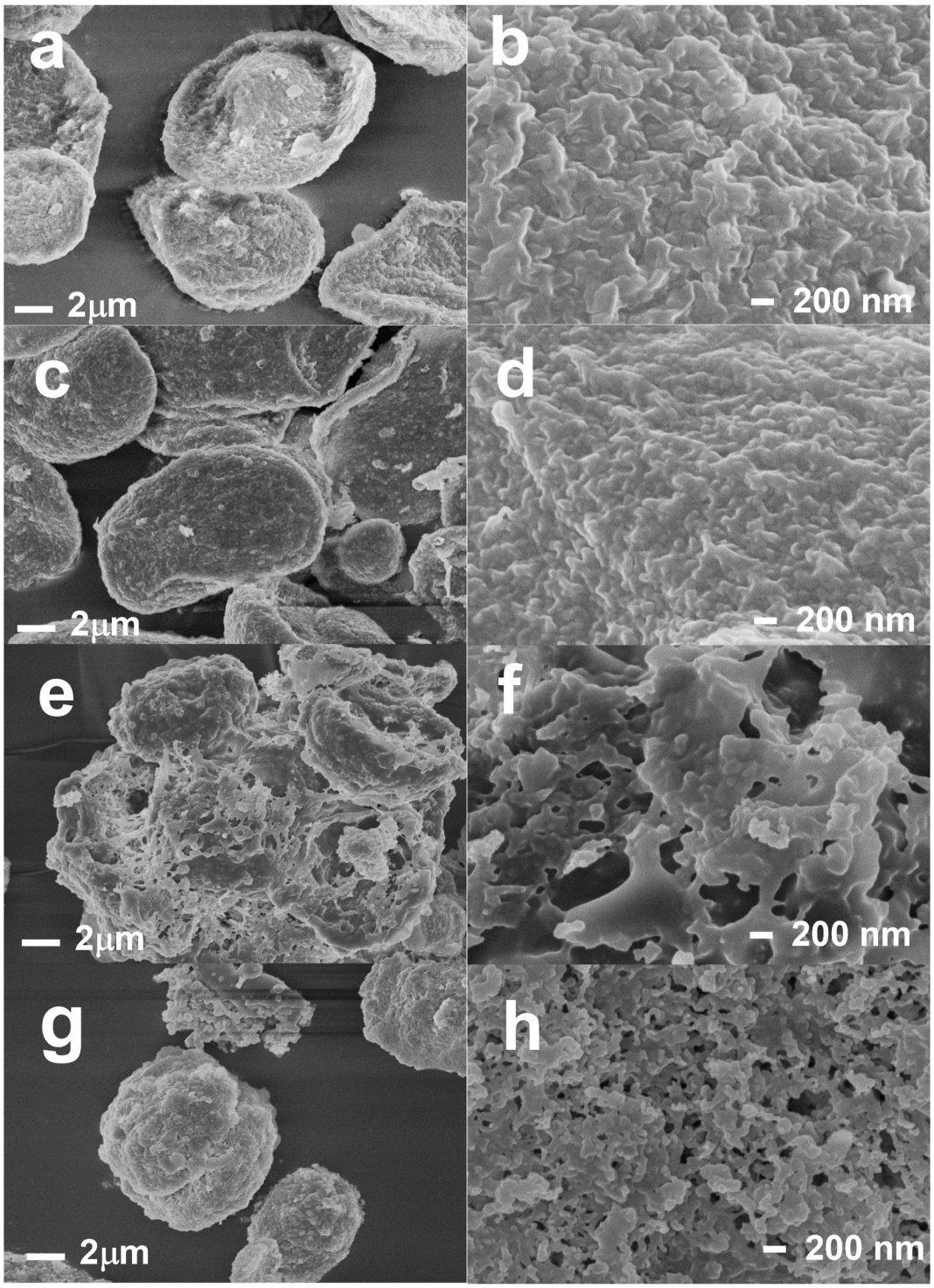

Fig. 3. SEM microphotoghraph of OLE enriched alginate-based microparticles (a,b: Alg; c,d: Alg/Pec; e,f: Alg/WPI; g,h: Alg/Cas).

at around 240 °C (*c*) with different magnitude for the two systems appeared (Table 2, Fig. 4a). This exothermic transition has been attributed to the polyelectrolytes degradation, due to dehydration, depolymerization and oxidative reactions (Belščak-Cvitanovic et al., 2016). The absence of this transition for CAS_Ingr, WPI_Ingr and OLE_Ingr suggests the specific involvement of polysaccharides in the reaction, as already supposed by other authors, who attributed this phenomenon to Maillard reaction and/or carbohydrates decomposition and proteins denaturation (Pugliese et al., 2016, 2019). The enthalphy of the exothermic c transition was about four times higher for Alg_Ingr than Pec_Ingr (Table 2). Cas_Ingr and WPI_Ingr revealed a more complex thermal behaviour (Fig. 4a). In detail, both Cas_Ingr and WPI_Ingr showed a glass transition (*d*) with Ton around 182 and 208 °C, respectively (Table 2). Cas_Ing showed also a second Tg (*e*) starting at around 228 °C and characterized by a signal change of only 0.12 W/g, while WPI_Ingr displayed an endothermic transition (*f*) with a maximum at around 246.6 °C. Glass transitions of the protein's amorphous fractions have been already observed by other authors in sodium caseinate and whey protein isolates samples, even if they were generally peaked at lower temperatures (Pugliese et al., 2016, 2019). For WPI_Ingr the

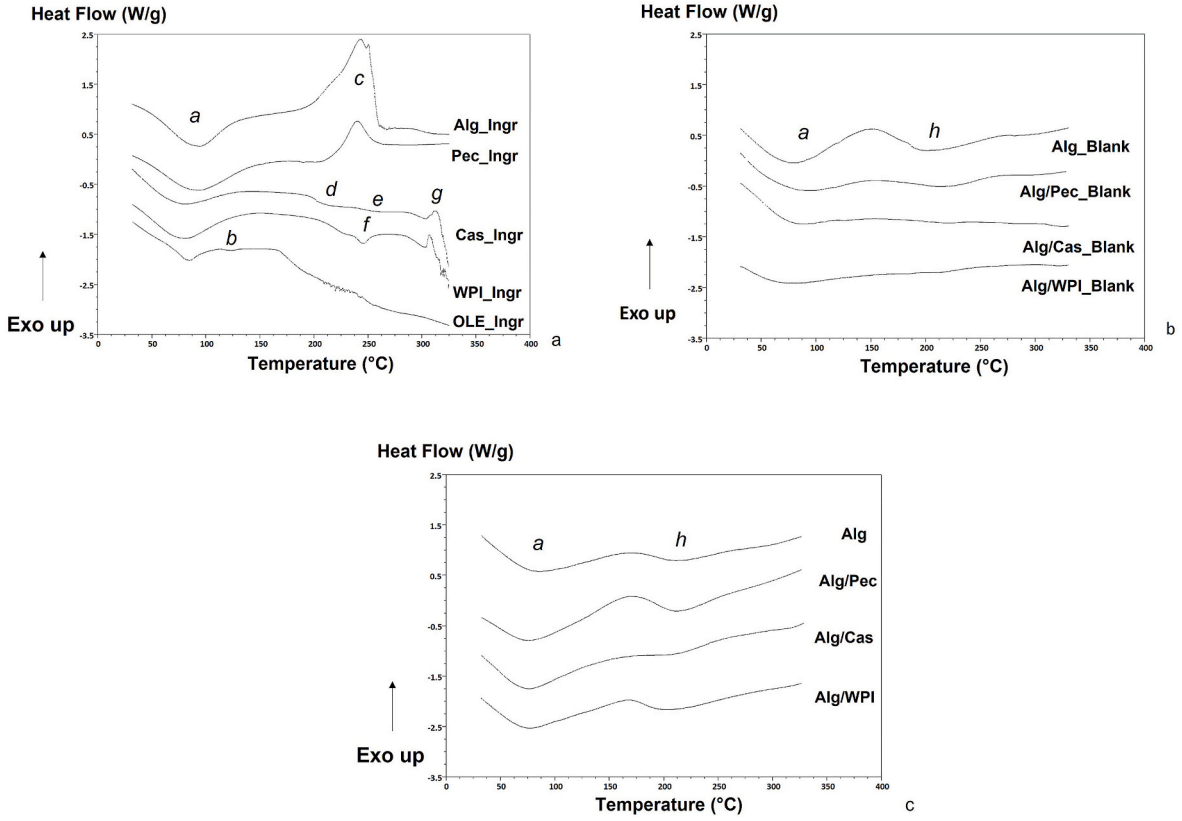

Fig. 4. DSC curves of a) ingredients before gelation; b) blank microbeads; c) OLE enriched microbeads.

presence of the endothermic first order transition (*f*) may be associated with the melting (denaturation) of the protein ordered regions. During processing, such as drying, not necessarily a protein native structure undergoes a complete denaturation towards fully amorphous structure; residual protein secondary structures, such as α-helices and β-sheets can be retained. When studied by DSC, the thermally induced denaturation of these residual ordered structures is observed as an endothermic peak (Bier et al., 2014). The physical state of a powder determines differences in physicochemical properties, chemical stability, water solubility, hygroscopy, flow properties, and compatibility. The exothermic peaks observed around 300 °C (*g*) for both Cas_Ingr and WPI_Ingr indicate thermal degratation of the samples.

Fig. 4b reports the thermal curves of the freeze dried blank microbeads. For all the systems, the first endothermic peak (*a*), previously associated to water loss, was still visible after gelation along with a second endothermic event (*i*), at around 200 °C. The latter event may be a result of the crosslinkage disruption, as stated by Pillay and Fassihi (1999). The presence of a single endotermic peak indicates depolimerization of a homogeneous mixture, even for the systems composed by two polymers. The shift of the *i* peak toward higher temperatures for the binary systems (Table 3) could be attributed to reinforcement in the alginate matrix with the addition of the other polymers (Lupo et al., 2015; Vallejo-Castillo et al., 2020). Moreover, the melting enthalphy of peak *i* resulted higher for Alg_Blank and Pec_Blank, suggesting the formation of more stable bonds. This assumption is supported by the observations made by FTIR on the same matrices in our previous published paper (Flamminii et al., 2020a), in which a significant shift in all the regions of the spectrum was observed when different polymers were added to alginate, demonstrating a change of hydrogen-bonding and carbohydrate network interactions.

No decomposition peaks at high temperatures were observed for all the systems, indicating the higher thermal stability of the egg-box structure (Belščak-Cvitanovic et al., 2016).

Fig. 4c reports the thermal curves of the freeze dried microbeads loaded with OLE. The two endothermic transitions, *a* and *h*, were also visible for these samples; on the other hand the melting peak observed for OLE_Ingr (*b*) was not detected anymore. The *h* enthalphy of Alg/Cas and Alg/WPI resulted higher for the enriched beads in comparison to the blanks (Tables 3 and 4), indicating the formation of new bonds with the OLE molecules. In general, the lower the enthalpy, the lower the interaction among the molecules. Such statement is confirmed in this study by the values of enthalpy of peak h (Table 4), which follow the same trend as the molecules retention values (Table 1). The modification of the peak size and shape after encapsulation, as well as the disappearance of the typical OLE_Ingr peak, suggest the occurrence of encapsulation. It is believed that the bioactive molecules, being well dispersed throughout the matrices, melted together with the encapsulation polymers (peak *h*). An improved thermal stability of the bioactive compounds may also be hypothesized (Vallejo-Castillo et al., 2020). These assumptions confirm what have been reported in our previous study, in which shift of the FTIR spectra was observed as a consequence of OLE encapsulation: in that case, we suggested that the molecular interactions between OLE and the encapsulating polymers were mostly formed via hydrogen bonding; moreover, also from that analysis, OLE seemed to interacted more with the carbohydrate moiety with respect to the protein one (Flamminii et al., 2020a). In particular, the polymers-polyphenols interaction seems to be related to the specific chemical composition of the molecules; indeed, this seems confirmed by the fact that Alg showed a higher interaction with Hydroxytyrosol, while Alg/Pec revealed a higher affinity with Oleuropein and Verbascoside (section 3.1). Further analyses are thus needed to deepen the physichemical mechanism underpinning the encapsulation of each single compound. The exothermic transition related to thermal degradation was not more visible in the considered range of temperatures, confirming the thermal stability of the systems.

Table 2
Thermal parameters obtained from the thermograms of the powder ingredients before gelation.

Ingredients	*Thermal transitions*		
	a (endo)		
	Ton	Tp	ΔH
Estr_Ingr	30.2 ± 0.5[a]	85.8 ± 0.8[b]	61.1 ± 9.9[d]
Alg_Ingr	30.4 ± 0.2[a]	88.3 ± 3.9[ab]	173.5 ± 22.5[c]
Pec_Ingr	29.4 ± 0.8[a]	89.0 ± 3.1[a]	268.3 ± 28.8[a]
Cas_Ing	29.8 ± 0.2[a]	80.1 ± 1.3[c]	181.9 ± 9.4[c]
WPI_Ingr	30.5 ± 0.3[a]	77.6 ± 2.7[c]	203.4 ± 16.0[b]
	***b* (endo)**		
	Ton	**Tp**	**ΔH**
Estr_Ingr	112.3 ± 0.5	123.5 ± 0.2	1.3 ± 0.4
	***c* (exo)**		
	Ton	**Tp**	**ΔH**
Alg_Ingr	188.1 ± 2.4[b]	244.4 ± 0.4[a]	361.5 ± 13.6[a]
Pec_Ingr	206.2 ± 0.5[a]	240.6 ± 0.3[b]	80.5 ± 4.7[b]
	***d* (*Tg*)**		
	Ton	**Tg**	**ΔCp**
Cas_Ing	182.2 ± 1.6[b]	200.9 ± 1.1[b]	0.27 ± 0.01[a]
WPI_Ingr	207.86 ± 1.8[a]	221.5 ± 0.6[a]	0.31 ± 0.03[a]
	***e* (*Tg*)**		
	Ton	**Tg**	**ΔCp**
Cas_Ing	228.4 ± 2.1		0.12 ± 0.01
	***f* (*endo*)**		
	Ton	**Tp**	**ΔH**
WPI_Ingr	236.6 ± 0.4	246.6 ± 0.1	9.2 ± 1.1
	***g* (exo)**		
	Ton	**Tp**	**ΔH**
Cas_Ing	303.2 ± 1.0[a]	310.3 ± 2.3[a]	32.6 ± 9.2[a]
WPI_Ingr	305.7 ± 1.7[a]	309.9 ± 2.2[a]	11.6 ± 5.6[b]

Data are reported as means of three replicates ± standard deviation. Different letters in the same coloumn, related to the same transition, indicate significant differences between the samples ($p < 0.05$). Abbreviations: endo, endothermic transition; exo, exothermic transition; glass, glass transition; Ton, onset temperature of the transition (°C); Tp, temperature at the peak maximum (°C); ΔH, enthalpy variation (J/g); Tg, glass transition temperature (°C); ΔCp, heat capacity variation (W/g). Letters identify the thermal transitions of Fig. 4a.

Table 3
Thermal parameters obtained from the thermograms of the blank microbeads.

		Alg_ Blank	Alg/Pec_ Blank	Alg/Cas_ Blank	Alg/WPI_ Blank
a	**Ton**	30.7 ± 0.3[a]	30.6 ± 0.4[a]	30.5 ± 0.6[a]	31.2 ± 0.2[a]
endo	**Tp**	80.9 ± 2.3b[c]	87.6 ± 3.7[a]	85.0 ± 1.2[ab]	78.1 ± 1.9[c]
	ΔH	271.9 ± 18.0[a]	203.0 ± 20.8[b]	83.0 ± 6.3[c]	159.4 ± 35.6[b]
h	**Ton**	152.0 ± 1.2[c]	159.4 ± 12.7[bc]	168.5 ± 7.0[b]	191.5 ± 2.5[a]
endo	**Tp**	200.3 ± 2.8[c]	210.0 ± 4.3[b]	220.8 ± 0.6[a]	213.0 ± 3.5[b]
	ΔH	138.2 ± 6.4[a]	72.8 ± 43.2[b]	9.2 ± 3.2[c]	6.2 ± 1.3[c]

Data are reported as means of three replicates ± standard deviation. Different letters in the same raw indicate significant differences between the samples ($p < 0.05$). Abbreviations: Ton, onset temperature (°C); Tp peak temperature (°C); ΔH, enthalpy variation (J/g). Letters identify the thermal transitions of Fig. 4b and c.

3.4. Color

The analysis of color may provide useful informations for the potential application of microparticles as food ingredient without variations on the visual appearance of the final product. Changes in the colorimetric parameters of microparticles enriched with OLE and those related to free OLE, are reported as hue angle and chroma (Fig. 5). The encapsulation procedure significantly affected the colorimetric parametes ($p < 0.05$) of microparticles with respect to those of pure OLE that highlights the lowest hue angle (76°) and the highest croma (30), values that reflect a more brown/yellow colored powder. Irrespective of the

Table 4
Thermal parameters obtained from the thermograms of the OLE enriched microbeads.

		Alg	Alg/Pec	Alg/Cas	Alg/WPI
a	**Ton**	30.5 ± 0.7[a]	30.5 ± 0.3[a]	30.4 ± 0.1[a]	30.4 ± 0.1[a]
endo	**Tp**	88.1 ± 5.1[a]	76.9 ± 0.9[b]	76.9 ± 1.2[b]	75.4 ± 2.5[b]
	ΔH	263.2 ± 13.6[a]	282.9 ± 33.2[a]	255.9 ± 69.8[a]	243.3 ± 14.8[a]
h	**Ton**	171.4 ± 2.5[a]	173.0 ± 1.5[a]	174.6 ± 3.3[a]	170.9 ± 1.1[a]
endo	**Tp**	214.0 ± 3.9[a]	209.4 ± 5.4[a]	211.7 ± 1.1[a]	201.3 ± 1.8[b]
	ΔH	47.0 ± 10.0[ab]	67.0 ± 12.3[a]	25.7 ± 4.9[c]	37.1 ± 10.8[bc]

Data are reported as means of three replicates ± standard deviation. Different letters in the same raw indicate significant differences between the samples ($p < 0.05$) following the relation a>b > c. Abbreviations: Ton, onset temperature (°C); Tp peak temperature (°C); ΔH, enthalpy variation (J/g). Letters identify the thermal transitions of Fig. 4b and c.

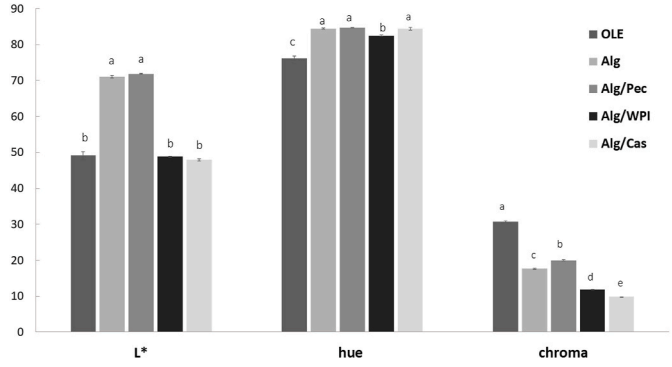

Fig. 5. Colorimetric parameters as lightness (L*), hue angle and chroma, of OLE enriched microparticles and pure OLE. Different letters for the same parameter indicate significant differences at a probability levele of $p < 0.05$.

composition, all the beads showed higher hue angle and lower chroma when compared to the extract, indicating powders with a reduced yellow/brown color than the pure OLE. Considering the results related to the microcapsules, matrix composition did not affect the hue angle values except when WPI was used as co-structurant. On the contrary, chroma resulted significantly affected by the type of polymer used ($p < 0.05$), following the relation Alg/Pec > Alg > Alg/WPI > Alg/Cas.

The systems enriched with proteins determined a reduction of 60–70% of the chroma values in comparison to that of pure OLE. This result may be associated to the initial color of both WPI and sodium caseinate powders used as co-structurant ingredients in the encapsulation procedures as also confirmed by the colorimetric indices of the same blank systems that resulted in lower a* and b* values (*data not shown*).

OLE powder is charachterized by the presence of colored apolar compounds such as chlorophyll and derivatives or flavonols like luteolin, naturally present in olive leaves (Flamminii et al., 2019). It has been proven that saccharides with α-(1,4) glycoside bonds generate apolar surfaces, increasing their ability to bind apolar molecules (Sundari and Balasubramanian, 1997). Thus, since pectin has α-(1,4) bonds, it is expected to interact and bind a higher fraction of these apolar pigments and therfore lead to a lower reduction of chroma value than pure OLE. Our results are in accordance to the results reported for OLE encapsulated in matrices at different matodextrins/trehalose ratio, which resulted to play a significant role in the color of the final powders (González-Ortega et al., 2020). The interference of arabic gum on the color of anthocyanin loaded spray-dried microparticles was also reported by other authors (da Silva Carvalho et al., 2016).

4. Conclusions

The findings of this study revealed that emulsification internal ionotropic gelation, by using alginate in combination with pectin, sodium caseinate or whey protein isolate appeared as a promising technique for the microencapsulation of olive leaf phenolic extracts, complementing the results of our previous preliminary research with the help of both microstructural and thermal evaluation.

Olive leaf polyphenols resulted differently retained by the explored encapsulation materials. Alginate/Pectin microcapsules resulted in general the most efficient for the encapsulation of this class of molecules, being the protein systems the less efficient, especially when caseins were used. The color measurement showed higher lightness for Alg and Alg/Pec in comparison to OLE, suggesting a higher suitability of these systems when used as ingredients in food formulations, thanks to the lower impact on the color of the finished products.

The DSC results suggest a higher degree of physicochemical interactions between olive leaf polyphenols with the Alg/Pec polymers, in comparison to the other studied systems. Thermal analysis also revealed the positive effect of gelation on the physicochemical and thermal stability of both OLE and pure ingredients.

In conclusion, this work explores the possibility to convert olive by-products into high added-value ingredients, in the form of polyphenol-loaded capsules, to be exploited in food matrices, especially the ones that undergo high thermal treatments as bakery products.

Funding

This research was supported by AGER 2 Project – "S.O.S – Sustainability of the Olive-Oil System" – grant no. 2016–0105.

CRediT authorship contribution statement

Federica Flamminii: Conceptualization, Methodology, Formal analysis, Data curation, Writing – original draft, preparation. **Maria Paciulli:** Conceptualization, Methodology, Formal analysis, Data curation, Writing – original draft, preparation. **Alessandro Di Michele:** Formal analysis. **Paola Littardi:** Formal analysis. **Eleonora Carini:** Resources, Writing – review & editing. **Emma Chiavaro:** Conceptualization, Methodology, Resources, Writing – review & editing, Supervision, Funding acquisition. **Paola Pittia:** Resources, Writing – review & editing. **Carla Daniela Di Mattia:** Conceptualization, Methodology, Resources, Writing – review & editing, Supervision, Project administration, Funding acquisition.

Declaration of competing interest

The authors declare that they have no known competing financial interests or personal relationships that could have appeared to influence the work reported in this paper.

References

Belščak-Cvitanovic, A., Bušić, A., Barišić, L., Vrsaljko, D., Karlović, S., Špoljarić, I., Vojvodić, A., Mršić, G., Komes, D., 2016. Emulsion templated microencapsulation of dandelion (Taraxacum officinale L.) polyphenols and β-carotene by ionotropic gelation of alginate and pectin. Food Hydrocolloids 57, 139–152. https://doi.org/10.1016/j.foodhyd.2016.01.020.

Belščak-Cvitanović, A., Dordević, V., Karlović, S., Pavlović, V., Komes, D., Ježek, D., Bugarski, B., Nedović, V., 2015. Protein-reinforced and chitosan-pectin coated alginate microparticles for delivery of flavan-3-ol antioxidants and caffeine from green tea extract. Food Hydrocolloids 51, 361–374. https://doi.org/10.1016/j.foodhyd.2015.05.039.

Bier, J.M., Verbeek, C.J.R., Lay, M.C., 2014. Thermal transitions and structural relaxations in protein-based thermoplastics. Macromol. Mater. Eng. 299, 524–539. https://doi.org/10.1002/MAME.201300248.

Bušić, A., Belščak-Cvitanović, A., Vojvodić Cebin, A., Karlović, S., Kovač, V., Špoljarić, I., Mršić, G., Komes, D., 2018. Structuring new alginate network aimed for delivery of dandelion (Taraxacum officinale L.) polyphenols using ionic gelation and new filler materials. Food Res. Int. 111, 244–255. https://doi.org/10.1016/j.foodres.2018.05.034.

Ching, S.H., Bansal, N., Bhandari, B., 2017. Alginate gel particles – a review of production techniques and physical properties. Crit. Rev. Food Sci. Nutr. 57, 1133–1152. https://doi.org/10.1080/10408398.2014.965773.

Córdoba, A.L., Deladino, L., Martino, M., 2014. Release of yerba mate antioxidants from corn starch-alginate capsules as affected by structure. Carbohydr. Polym. 99, 150–157. https://doi.org/10.1016/j.carbpol.2013.08.026.

da Silva Carvalho, A.G., da Costa Machado, M.T., da Silva, V.M., Sartoratto, A., Rodrigues, R.A.F., Hubinger, M.D., 2016. Physical properties and morphology of spray dried microparticles containing anthocyanins of jussara (Euterpe edulis Martius) extract. Powder Technol. 294, 421–428. https://doi.org/10.1016/j.powtec.2016.03.007.

Difonzo, G., Russo, A., Trani, A., Paradiso, V.M., Ranieri, M., Pasqualone, A., Summo, C., Tamma, G., Silletti, R., Caponio, F., 2017. Green extracts from Coratina olive cultivar leaves: antioxidant characterization and biological activity. J Funct Foods 31, 63–70. https://doi.org/10.1016/j.jff.2017.01.039.

Elzoghby, A.O., Helmy, M.W., Samy, W.M., Elgindy, N.A., 2013. Novel ionically crosslinked casein nanoparticles for flutamide delivery: formulation, characterization, and in vivo pharmacokinetics. Int. J. Nanomed. 8, 1721–1732. https://doi.org/10.2147/IJN.S40674.

Fang, Z., Bhandari, B., 2010. Encapsulation of polyphenols – a review. Trends Food Sci. Technol. 21, 510–523. https://doi.org/10.1016/J.TIFS.2010.08.003.

Flamminii, F., Di Mattia, C., Nardella, M., Chiarini, M., Valbonetti, L., Neri, L., Difonzo, G., Pittia, P., 2020a. Structuring alginate beads with different biopolymers for the development of functional ingredients loaded with olive leaves phenolic extract. Food Hydrocolloids 108, 105849. https://doi.org/10.1016/j.foodhyd.2020.105849.

Flamminii, F., González-Ortega, R., Di Mattia, C.D., Perito, M.A., Mastrocola, D., Pittia, P., 2020b. Applications of compounds recovered from olive mill waste. In: Galanakis, Charis (Ed.), Food Waste Recovery- Processing Technologies, Industrial Techniques, and Applications. Elsevier-Academic Press, pp. 327–353. https://doi.org/10.1016/B978-0-12-820563-1.00006-8.

Flamminii, F., Di Mattia, C.D., Difonzo, G., Neri, L., Faieta, M., Caponio, F., Pittia, P., 2019. From by-product to food ingredient: evaluation of compositional and technological properties of olive-leaf phenolic extracts. J. Sci. Food Agric. 99, 6620–6627. https://doi.org/10.1002/jsfa.9949.

Ganje, M., Jafari, S.M., Dusti, A., Dehnad, D., Amanjani, M., Ghanbari, V., 2016. Modeling quality changes in tomato paste containing microencapsulated olive leaf extract by accelerated shelf life testing. Food Bioprod. Process. 97, 12–19. https://doi.org/10.1016/j.fbp.2015.10.002.

González-Ortega, R., Faieta, M., Di Mattia, C.D., Valbonetti, L., Pittia, P., 2020. Microencapsulation of olive leaf extract by freeze-drying: effect of carrier composition on process efficiency and technological properties of the powders. J. Food Eng. 285, 110089. https://doi.org/10.1016/j.jfoodeng.2020.110089.

Hassen, I., Casabianca, H., Hosni, K., 2015. Biological activities of the natural antioxidant oleuropein: exceeding the expectation - a mini-review. J Funct Foods 18, 926–940. https://doi.org/10.1016/j.jff.2014.09.001.

Jolayemi, O.S., Stranges, N., Flamminii, F., Casiraghi, E., Alamprese, C., 2021. Influence of free and encapsulated olive leaf phenolic extract on the storage stability of single and double emulsion salad dressings. Food Bioprocess Technol. 14, 93–105. https://doi.org/10.1007/s11947-020-02574-y.

Jyothi, N.V.N., Prasanna, P.M., Sakarkar, S.N., Prabha, K.S., Ramaiah, P.S., Srawan, G.Y., 2010. Microencapsulation techniques, factors influencing encapsulation efficiency. J. Microencapsul. 27, 187–197. https://doi.org/10.3109/02652040903131301.

Kurozawa, L.E., Hubinger, M.D., 2017. Hydrophilic food compounds encapsulation by ionic gelation. Curr Opin Food Sci 15, 50–55. https://doi.org/10.1016/j.cofs.2017.06.004.

Leong, J.Y., Lam, W.H., Ho, K.W., Voo, W.P., Lee, M.F.X., Lim, H.P., Lim, S.L., Tey, B.T., Poncelet, D., Chan, E.S., 2016. Advances in fabricating spherical alginate hydrogels with controlled particle designs by ionotropic gelation as encapsulation systems. Particuology 24, 44–60. https://doi.org/10.1016/j.partic.2015.09.004.

Li, Q., Duan, M., Hou, D., Chen, X., Shi, J., Zhou, W., 2021. Fabrication and characterization of Ca(II)-alginate-based beads combined with different polysaccharides as vehicles for delivery, release and storage of tea polyphenols. Food Hydrocolloids 112, 106274. https://doi.org/10.1016/j.foodhyd.2020.106274.

Li, Y., Lim, L.T., Kakuda, Y., 2009. Electrospun zein fibers as carriers to stabilize (-)-epigallocatechin gallate. J. Food Sci. 74, C233–C240. https://doi.org/10.1111/j.1750-3841.2009.01093.x.

Lu, W., Kelly, A.L., Miao, S., 2016. Emulsion-based encapsulation and delivery systems for polyphenols. Trends Food Sci. Technol. 47, 1–9. https://doi.org/10.1016/j.tifs.2015.10.015.

Lupo, B., Maestro, A., Gutiérrez, J.M., González, C., 2015. Characterization of alginate beads with encapsulated cocoa extract toprepare functional food: comparison of two gelation mechanisms. Food Hydrocolloids 49, 25–34. https://doi.org/10.1016/j.foodhyd.2015.02.023.

McClements, D.J., 2017. Designing biopolymer microgels to encapsulate, protect and deliver bioactive components: physicochemical aspects. Adv. Colloid Interface Sci. 240, 31–59. https://doi.org/10.1016/j.cis.2016.12.005.

Mohammadi, A., Jafari, S.M., Esfanjani, A.F., Akhavan, S., 2016. Application of nano-encapsulated olive leaf extract in controlling the oxidative stability of soybean oil. Food Chem. 190, 513–519. https://doi.org/10.1016/j.foodchem.2015.05.115.

Mourtzinos, I., Salta, F., Yannakopoulou, K., Chiou, A., Karathanos, V.T., 2007. Encapsulation of olive leaf extract in β-cyclodextrin. J. Agric. Food Chem. 55, 8088–8094. https://doi.org/10.1021/jf0709698.

Osojnik Črnivec, I.G., Poklar Ulrih, N., 2019. Nano-hydrogels of alginate for encapsulation of food ingredients. Biopolymer Nanostructures for Food Encapsulation Purposes. Elsevier, pp. 335–380. https://doi.org/10.1016/b978-0-12-815663-6.00013-6.

Ozkan, G., Franco, P., De Marco, I., Xiao, J., Capanoglu, E., 2019. A review of microencapsulation methods for food antioxidants: principles, advantages, drawbacks and applications. Food Chem. 272, 494–506. https://doi.org/10.1016/j.foodchem.2018.07.205.

Pacheco, C., González, E., Robert, P., Parada, J., 2018. Retention and pre-colon bioaccessibility of oleuropein in starchy food matrices, and the effect of microencapsulation by using inulin. J Funct Foods 41, 112–117. https://doi.org/10.1016/j.jff.2017.12.037.

Paulo, F., Santos, L., 2020. Deriving valorization of phenolic compounds from olive oil by-products for food applications through microencapsulation approaches: a comprehensive review. Crit. Rev. Food Sci. Nutr. 61, 920–945. https://doi.org/10.1080/10408398.2020.1748563.

Pillay, V., Fassihi, R., 1999. In vitro release modulation from crosslinked pellets for site-specific drug delivery to the gastrointestinal tract: I. Comparison of pH-responsive drug release and associated kinetics. J. Contr. Release 59, 229–242. https://doi.org/10.1016/S0168-3659(98)00196-5.

Pugliese, A., Paciulli, M., Chiavaro, E., Mucchetti, G., 2019. Application of differential scanning calorimetry to freeze-dried milk and milk fractions. J. Therm. Anal. Calorim. 137, 703–709. https://doi.org/10.1007/s10973-018-7971-7.

Pugliese, A., Paciulli, M., Chiavaro, E., Mucchetti, G., 2016. Characterization of commercial dried milk and some of its derivatives by differential scanning calorimetry. J. Therm. Anal. Calorim. 123, 2583–2590. https://doi.org/10.1007/s10973-016-5243-y.

Robert, P., Zamorano, M., González, E., Silva-Weiss, A., Cofrades, S., Giménez, B., 2019. Double emulsions with olive leaves extract as fat replacers in meat systems with high oxidative stability. Food Res. Int. 120, 904–912. https://doi.org/10.1016/j.foodres.2018.12.014.

Roselló-Soto, E., Koubaa, M., Moubarik, A., Lopes, R.P., Saraiva, J.A., Boussetta, N., Grimi, N., Barba, F.J., 2015. Emerging opportunities for the effective valorization of wastes and by-products generated during olive oil production process: non-conventional methods for the recovery of high-added value compounds. Trends Food Sci. Technol. 45, 296–310. https://doi.org/10.1016/J.TIFS.2015.07.003.

Sundari, C.S., Balasubramanian, D., 1997. Hydrophobic surfaces in saccharide chains. Prog. Biophys. Mol. Biol. 67, 183–216. https://doi.org/10.1016/S0079-6107(97)00016-3.

Tavakoli, H., Hosseini, O., Jafari, S.M., Katouzian, I., 2018. Evaluation of physicochemical and antioxidant properties of yogurt enriched by olive leaf phenolics within nanoliposomes. J. Agric. Food Chem. 66, 9231–9240. https://doi.org/10.1021/acs.jafc.8b02759.

Vallejo-Castillo, V., Rodríguez-Stouvenel, A., Martínez, R., Bernal, C., 2020. Development of alginate-pectin microcapsules by the extrusion for encapsulation and controlled release of polyphenols from papaya (Carica papaya L.). J. Food Biochem. 44, e13331 https://doi.org/10.1111/jfbc.13331.